Journal of Catalysis **196,** 66–72 (2000)
doi:10.1006/jcat.2000.3017, available online at http://www.idealibrary.com on IDEAL®

A Novel Fluidized Bed Technique for Measuring UV Raman Spectra of Catalysts and Adsorbates

Yek Tann Chua and Peter C. Stair[1]

Department of Chemistry, Northwestern University, 2145 Sheridan Road, Evanston, Illinois 60208

Received March 13, 2000; accepted August 3, 2000

A novel "fluidized bed" (FB) technique for measuring UV Raman spectra of catalysts and adsorbates has been developed to minimize thermal degradation and possible photodecomposition of adsorbates by UV radiation. UV Raman spectra were measured for naphthalene, benzene, and pyridine adsorbed in zeolite H-USY. When measurements were performed on samples in the form of a stationary or spinning disc, the Raman spectra show the presence of "coke," a typical end product of heating and photochemistry. In contrast, the Raman peaks of the unreacted adsorbates dominate spectra measured using the FB apparatus. An *in situ* FB reactor was constructed and the UV Raman spectrum of *n*-heptane in zeolite H-ZSM-5 was measured. These results indicate that the FB technique is a promising method for measuring UV Raman spectra of catalysts and adsorbates.

Key Words: **fluidized bed technique; UV Raman spectra; catalysts; adsorbates.**

INTRODUCTION

Raman spectroscopy is a powerful tool that has wide application in the field of heterogeneous catalysis. For example, it has been used to characterize the molecular structure of supported metal oxides (1, 2) and to study the dynamics of molecular sieves (3, 4) and has contributed to an understanding of the formation of zeolites (5, 6). It is also capable of detecting reaction intermediates (7, 8), even transient species under certain conditions (9). However, Raman spectra measured using visible wavelength radiation are often plagued by strong fluorescence that masks the much weaker Raman peaks. The origin of fluorescence is usually attributed to traces of fluorescent heavy metal ions, the presence of hydroxyl groups on oxide surfaces, or hydrocarbon impurities (10, 11), which, in many cases, are a side product of hydrocarbon catalysis. Fluorescence can be avoided by using either near-IR (12) or UV (13) lasers to record Raman spectra. Measuring Raman spectra in the UV offers attractive advantages over spectra taken with near-IR radiation. Because of the frequency dependence in normal Raman spectroscopy, the intensity of a Raman peak is stronger under UV excitation than under near-IR radiation. In addition, thermal luminescence from samples at elevated temperatures does not interfere with UV Raman measurements. For species that absorb UV radiation, UV resonance Raman spectroscopy may increase detection sensitivity. In the past few years, our group has successfully used UV Raman spectroscopy to study a wide variety of catalytic systems and in all cases, fluorescence was completely avoided (14–16).

For materials that absorb laser radiation, heating may lead to thermal degradation of the samples. Spinning the sample in the form of a self-supporting disc (17) or cooling the sample (18) can be used to reduce heating. However, these methods are ineffective when the sample decomposes upon absorbing radiant energy. Interference from photodecomposition is particularly severe when the photo products build up in the region exposed to the laser beam. To minimize interference from both thermal degradation and photodegradation, a novel FB technique has been developed for measuring UV Raman spectra of catalysts and adsorbates. In this paper, the method will be described and the recording of adsorbate UV Raman spectra with little or no interference from photodecomposition and/or thermal degradation will be demonstrated. The method has been used to measure the UV Raman spectra of adsorbates in the important industrial zeolite catalysts H-USY and H-ZSM-5. We will also make some comments regarding the strengths and weaknesses of UV, visible, and near-IR Raman spectroscopies.

METHODS

Raman Spectrometer

Figure 1 shows a schematic diagram of the UV Raman instrument. The laser source is a Lexel 95 SHG (Second Harmonic Generation) laser (19) equipped with an intracavity nonlinear crystal, BBO (β-barium borate, BaB_2O_4), that frequency doubles visible radiation into midultraviolet.

[1] To whom correspondence should be addressed. Fax: (847) 467 1018. E-mail: pstair@nwu.edu.

0021-9517/00 $35.00

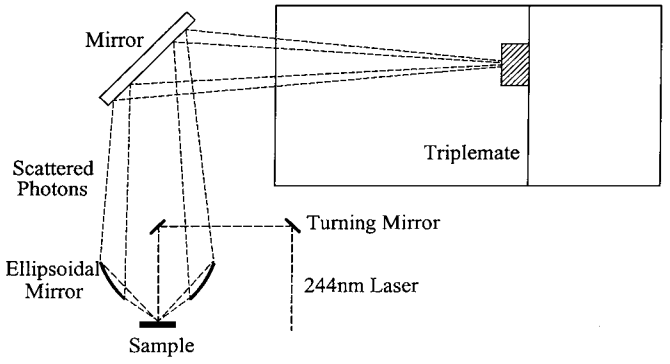

FIG. 1. Schematic diagram of UV Raman spectrometer.

An ellipsoidal mirror (20) is used to collect and focus the scattered photons into a Spex 1877 triple grating spectrometer. This mirror has an $AlMgF_2$ coating and collects light at polar angles from 39.9° to 66° and all azimuthal angles about the surface normal. Its minimum effective f/n is 0.22 and the solid angle of collection is 2.3 sr. The minimum blur circle at the second focus was measured to be 460 μm. This mirror is positioned so that the major axis of its parent ellipsoid is vertical. Scattered light from the ellipsoidal mirror reflects off a 6-in. mirror (21), 80% reflectance at 244 nm, before entering the spectrometer. The six spherical mirrors in the spectrometer received a broadband UV-enhanced coating optimized for 250 nm (22). The other components of the Raman instrument are described in detailed elsewhere (16).

Methods of Recording UV Raman Spectra: Fluidized Bed Technique

With the exception of liquids, all UV Raman spectra were measured using 244-nm radiation with a power of $\leq$2 mW. Measurements were performed on stationary powders or discs, on samples in the form of spinning self-supporting discs of 1.5 cm in diameter ($\sim$2000 revolutions per minute), and on a FB apparatus (Fig. 2). The first FB experiments were performed on powders placed on top of the fritted disc in a standard filter funnel (4- to 5.5-μm-size pores). In a typical experiment about 200 mg of powdered sample was loaded on the fritted disc. Flowing nitrogen gas was piped into the stem of the filter funnel at a rate ($\sim$20 cm^3/s) that produced constant tumbling and stirring of the powder without lifting the bed off the fritted disc. To facilitate the tumbling motion, an electromagnetic shaker that vibrated at $\sim$60 Hz (23) was also used. Over time zeolite particles tend to adhere to one another, forming millimeter-sized clumps that did not tumble easily. To overcome this problem, the powder was first pressed into wafers (pressure $<$ 1 ton/cm^2) and then subsequently ground into smaller pieces. The ground sample was sieved and particles

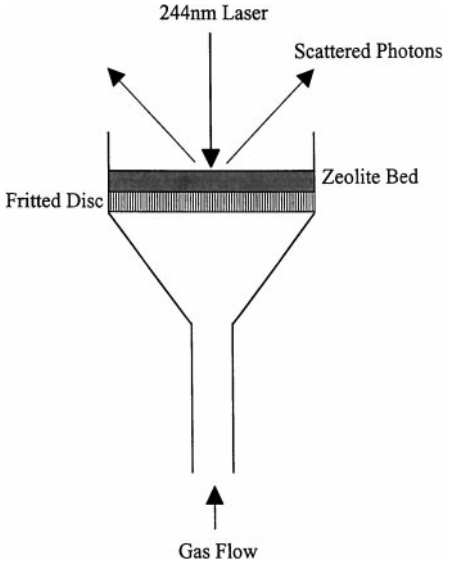

FIG. 2. A fritted funnel for fluidized bed experiments.

having sizes from 177 to 250 μm or 125 to 177 μm were selected for use in FB experiments. The naphthalene/H-USY sample was provided by Amoco Oil Co. The benzene/H-USY and pyridine/H-USY samples were prepared in this laboratory by dosing the respective organics into H-USY after the zeolite was calcined at 500°C in oxygen.

In Situ Fluidized Bed Reactor

Figure 3 shows a schematic diagram of an *in situ* FB reactor. A stainless steel porous disc (40-μm-size pores) (24) is positioned near the top of a stainless steel tube. The catalysts are placed on top of the porous disc. The tube is surrounded by a cylindrical quartz cover. Gases are introduced into the reactor with the direction of gas flow shown in the

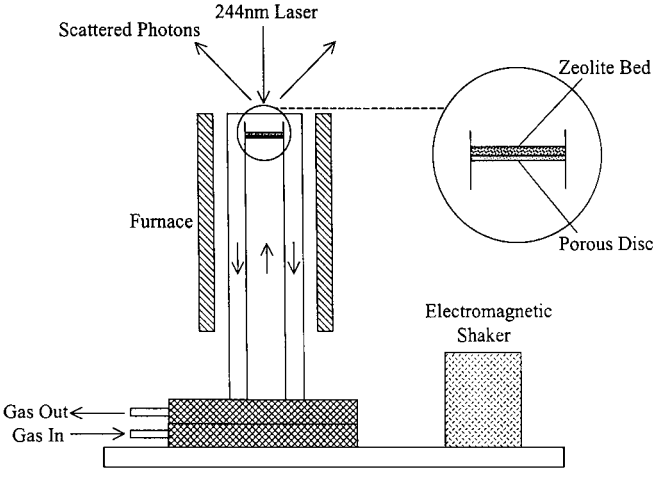

FIG. 3. Schematic diagram of the *in situ* fluidized bed reactor.

diagram. A cylindrical furnace surrounds the reactor. The temperature of the catalyst is measured by a thermocouple inserted from the bottom of the reactor and controlled by a temperature controller (25). The reactor is securely attached to a baseplate that also holds an electromagnetic shaker to facilitate tumbling of the catalyst particles. The laser beam is focused vertically down onto the top surface of the powder bed, and the scattered photons are collected by the ellipsoidal mirror.

The *n*-heptane/H-ZSM-5 sample was prepared by first calcining the zeolite in oxygen at 500°C, followed by cooling to room temperature and introduction of *n*-heptane in a stream of helium. The sample was purged in helium to remove physisorbed *n*-heptane and its UV Raman spectrum was then recorded.

RESULTS AND DISCUSSION

Before the FB technique was developed, Raman spectra in our laboratory were measured from stationary powders and pellets or from spinning discs. For the stationary sample, the laser is focused onto a small area of the sample. This results in thermal degradation (which may be accompanied by photodecomposition) of many organic adsorbates to produce "coke." Here coke refers to a form of amorphous carbon produced by the thermal degradation and/or photodecomposition of the adsorbates unless stated otherwise. With a spinning disc, the laser traverses the same circular path many times during the measurement of a Raman spectrum. In many cases this is an effective method for avoiding laser-induced heating (17, 26). However, in nearly all UV Raman spectra recorded using this method coke peaks were observed. This indicates that some compounds along the circular path have undergone photodegradation to form coke during the measurement. While the extent and rate of coke formation vary from sample to sample, strong coke peaks are present in most spectra.

For measurements using stationary and spinning discs, the laser beam interacts with only a small fraction of the total sample. The FB method, described under methods, makes it possible to expose more of the sample during a measurement, thereby reducing the buildup of decomposition products. Moreover, if particles in the FB move through the laser beam path at a much faster rate than the formation of coke, then the formation of coke will not interfere with the measurement of UV Raman spectra. For particles to move rapidly against one another with minimal resistance, the ideal shape is spherical. The zeolite particles used for FB experiments are not perfectly spherical (Fig. 4), but they are sufficiently rounded to allow efficient mixing during a FB experiment. Small particles (<125 μm) tend to stick together while large ones (>250 μm) require a higher gas flow for sufficient motion. The following paragraphs and figures show that UV Raman spectra of adsorbates nearly free of decomposition can be obtained using this new measurement method.

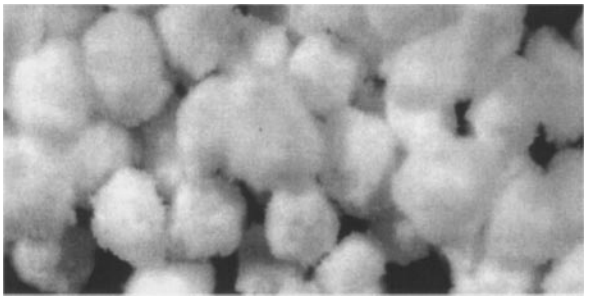

FIG. 4. Optical micrograph of zeolite particles (125 to 177 μm) used in fluidized bed experiments. This micrograph was taken using a Wild microscope (Heerbrugg, Switzerland).

Figures 5, 6, and 7 show the respective UV Raman spectra of naphthalene, benzene, and pyridine adsorbed in zeolite H-USY. These organic compounds absorb 244-nm radiation (27). Among the samples measured in this laboratory, they were found to be quite sensitive to UV irradiation and rapidly formed coke. Figure 5 shows the spectra of naphthalene as a neat compound (spectrum 5a) and

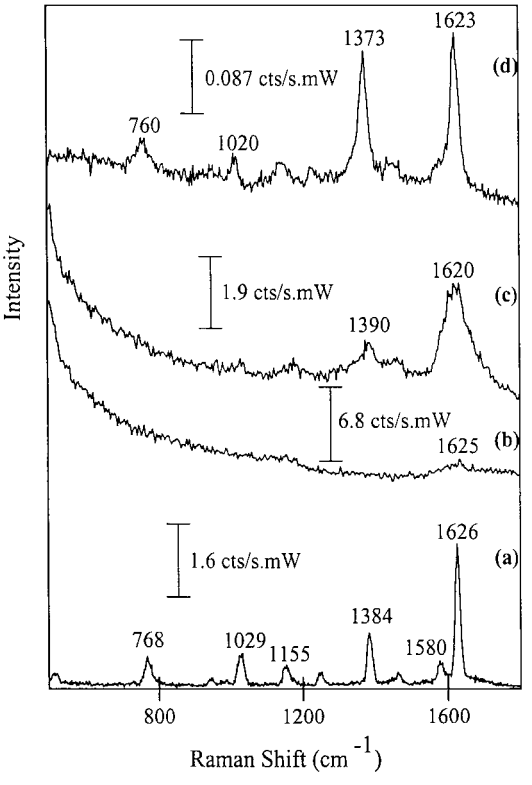

FIG. 5. (a) Spectrum of naphthalene recorded on a spinning disc. Laser power, 0.2 mW. Collection time, 1000 s. (b) Spectrum of naphthalene/H-USY recorded on a stationary disc. 0.3 mW; 300 s. (c) Spectrum of naphthalene/H-USY recorded on a spinning disc. 0.3 mW; 600 s. (d) Spectrum of naphthalene/H-USY recorded using the fluidized bed apparatus. 1.5 mW; 3600 s.

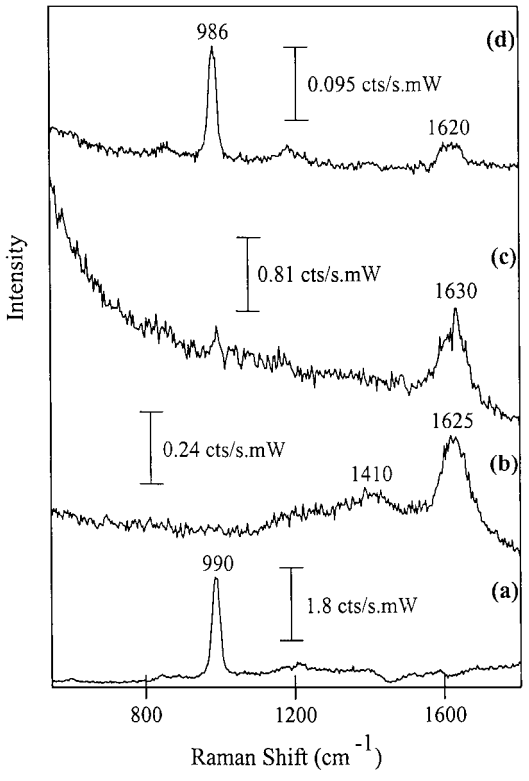

FIG. 6. (a) Spectrum of liquid benzene. Laser power, 5 mW. Collection time, 120 s. (b) Spectrum of benzene/H-USY recorded on a stationary powder. 2 mW; 900 s. (c) Spectrum of benzene/H-USY recorded on a spinning disc. 2 mW; 180 s. (d) Spectrum of benzene/H-USY recorded using the fluidized bed apparatus. 2 mW; 3600 s.

adsorbed in H-USY recorded using a stationary disc (spectrum 5b), a spinning disc (spectrum 5c), and the FB method (spectrum 5d). The Raman shifts for peaks from neat naphthalene measured using UV excitation compare well with those reported using visible radiation (28). The relative intensities, however, differ due to resonance enhancement. The peak at 1626 cm^{-1}, assigned to a CC stretch, is resonance enhanced under 244-nm excitation. Only a small peak at 1625 cm^{-1} is observed in spectrum 5b. This peak can be attributed to coke as it is typically seen in the UV Raman spectra of chemically produced coke on used catalysts (14, 15). The peak at 1620 cm^{-1} and a broad peak from 1300 to 1550 cm^{-1} in spectrum 5c are signature coke peaks. From our previous work on coke formation in zeolites (14, 15), it was concluded that the coke structure was sensitive to reaction temperature. Changes in coke structure were indicated by shifts of the coke peaks in the Raman spectra. The decrease by 5 cm^{-1} of the 1625-cm^{-1} Raman peak suggests that the structures of the coke in the stationary and spinning disc samples are different. Since the degree of local heating by the laser beam (hence the extent of naphthalene thermal decomposition) and the extent of naphthalene photodegradation in the samples are expected to be different, a change in the coke structure is not unexpected.

Spectrum 5d, measured using the FB method, clearly shows that the dominant peaks are those of the undecomposed molecular adsorbate. The peaks in spectrum 5d are shifted 3 to 11 cm^{-1} from those of neat naphthalene. These shifts are attributed to interactions between naphthalene molecules and the zeolite walls and possibly also water molecules that are adsorbed in the zeolite. The possibility that the shifts are due to laser-induced heating was ruled out by comparing spectrum 5d measured at 1.5 mW to a spectrum measured at 7 mW. If the peak shifts were produced by laser-induced heating, the magnitude of the shift should correlate with the incident laser power. Instead, the spectra were found to be identical to within experimental error.

Figure 6 shows the UV Raman spectra of benzene in H-USY. The strong peak at 990 cm^{-1} assigned to a symmetric ring breathing mode (28) is barely detectable in spectra 6b and 6c. Intense coke peaks are present in both spectra. The spectrum recorded with the FB method shows that the dominant species is benzene. The UV Raman spectra of pyridine in H-USY are shown in Fig. 7. Again, sample degradation is minimized in the spectrum recorded with the FB method. The Raman peaks at 985 and 1020 cm^{-1} of

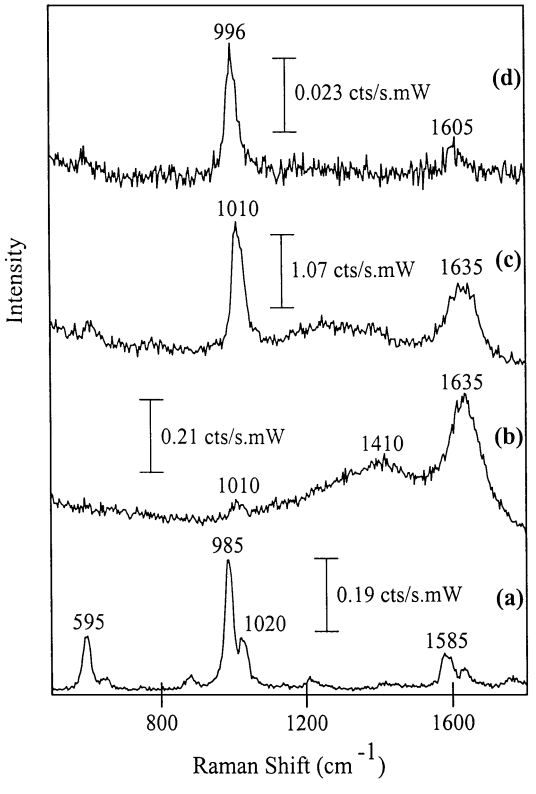

FIG. 7. (a) Spectrum of liquid pyridine. Laser power, 17 mW. Collection time, 120 s. (b) Spectrum of pyridine/H-USY recorded on a stationary powder. 1.6 mW; 1500 s. (c) Spectrum of pyridine/H-USY recorded on a spinning disc. 2 mW; 120 s. (d) Spectrum of pyridine/H-USY recorded using the fluidized bed apparatus. 1.4 mW; 4000 s.

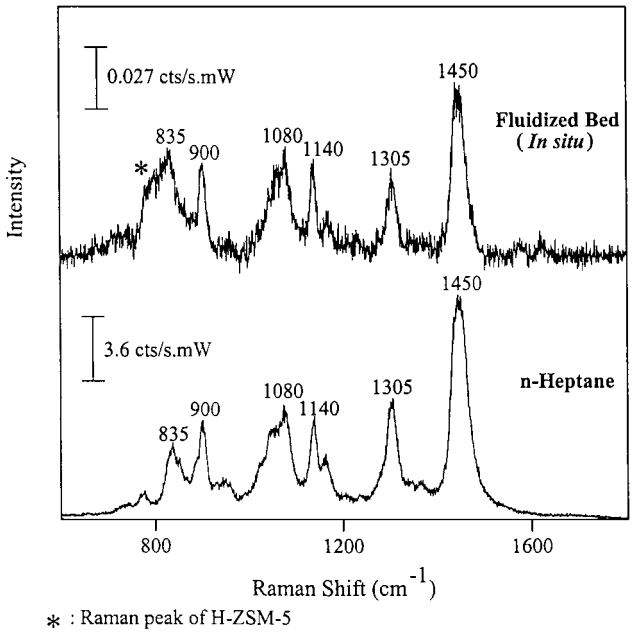

FIG. 8. Top spectrum: *n*-heptane/H-ZSM-5 recorded using the *in situ* fluidized bed reactor. Laser power, 2 mW. Collection time, 7000 s. Bottom spectrum: Liquid *n*-heptane. 2 mW; 60 s.

liquid pyridine apparently have merged into an unresolved peak (996 cm^{-1}) in spectrum 7d. This may be due to the interactions between the pyridine molecules, the zeolite, and/or adsorbed water.

From these examples, the FB method is shown to be a promising technique for measuring UV Raman spectra of catalytic materials. Recently, a reactor for performing *in situ* experiments was constructed. The Raman spectrum of *n*-heptane adsorbed in zeolite H-ZSM-5 recorded using this reactor is shown in Fig. 8. The spectrum shows that molecular *n*-heptane is the dominant species in H-ZSM-5. The similarity between liquid phase and adsorbed *n*-heptane spectral peak positions, band widths, and relative peak intensities suggests that the interactions between *n*-heptane molecules and the zeolite walls are similar to the interactions between molecules in the liquid phase. Small peaks attributable to coke are detectable. Although *n*-heptane has negligible absorption at 244 nm (29), the small coke peaks in the Raman spectrum suggest that the zeolite aids the photodecomposition of the adsorbate. It was reported that some zeolites assist the photochemical reactions of reagents by altering the electronic absorption profile of the adsorbed complex (30). Also silica and some metal oxides have been found to be photocatalytically active under UV radiation (31, 32). Certain active sites on these materials have been proposed to be responsible for the photochemical reactions of the organic adsorbates.

In our experiments, the laser beam is focused to ~40 μm (33) on the sample. Due to the entrance slitwidth of the spectrometer that we have used in our experiments (200 μm, which gives a spectral resolution of ~10 cm^{-1}) and the magnification of our ellipsoidal mirror (9.8 to 24.6), only scattered light from the central segment (~40 μm by ~8 μm) of the focused beam will enter the spectrometer. The depth of field of our ellipsoidal mirror is ~400 μm (34). Therefore, only scattered light within the volume with sides of ~40 μm by ~8 μm by ~400 μm will enter the spectrometer. However, at any instant during a FB experiment, only part of a particle or none at all is located in this volume. This causes the Raman count rate to be lower for a FB measurement than for a stationary or spinning disc. Typically the Raman count rate from a FB measurement was found to be 15 to 20% of that from a spinning sample. Since the particle density in the FB is lower than in a compressed disc, it is not practical to use Raman collection optics with a very small collection volume because the particles must be within this small volume in order to detect the Raman scattered photons.

The FB method itself provides the means to distinguish between laser-induced chemical reactions and catalyzed chemical reactions in a sample. The measured FB spectra are a time average of the steady state sample composition in the volume excited by the laser and imaged into the spectrometer. The steady state sample composition in this volume is determined by the balance between the rate of sample decomposition and the rate of fresh sample entering the laser beam. Assuming that the rate of laser-induced chemistry is correlated to the laser power, the contribution of the laser-induced chemistry to a measured spectrum can be changed by changing the incident laser power. In the FB experiments reported here, the laser power was typically low ($\leq$2 mW). As indicated above, the UV Raman spectrum of adsorbed naphthalene is unchanged after the laser power is increased to 7 mW. For pyridine/H-USY, the spectrum remains the same when the laser power is increased from 2 to 20 mW. For benzene/H-USY, however, the peak at ~1600 cm^{-1} increases with increasing laser power. These spectra suggest the laser-induced photochemistry is much more severe for benzene than naphthalene and pyridine.

Raman spectroscopy excited by visible and near-IR radiation has been used successfully to study the properties of catalytic materials. However, there are situations where it would be more advantageous to use UV Raman spectroscopy. In the following paragraphs, the strengths and weaknesses of UV, visible, and near-IR spectroscopies will be compared, and possible scenarios described when one technique is preferred to the other methods for catalytic studies.

When there is sample fluorescence that cannot be removed by physical or chemical means or because of reaction conditions that produce fluorescing species, eg., coke, UV or near-IR Raman spectroscopy can be used to circumvent this problem. For experiments where the samples must

be measured at high temperatures ($\gtrsim$150°C) (35), thermal blackbody radiation interferes with near-IR Raman spectroscopy. Thus UV Raman spectroscopy is the method of choice for *in situ* measurements at elevated temperatures when fluorescence from the catalyst or from carbonaceous deposits is unavoidable.

When high resolution is desired ($\lesssim 2\ cm^{-1}$), near-IR Raman or visible Raman spectroscopy is superior to UV Raman spectroscopy (1, 36). At present, the best resolution that has been achieved for UV Raman spectroscopy in our laboratory is $\sim 10\ cm^{-1}$.

Because of the frequency dependence (ν^4) under normal Raman scattering conditions, near-IR Raman spectroscopy has the lowest intrinsic sensitivity, and UV Raman spectroscopy has the highest. However, for samples that are transparent in the visible and near-IR but absorb strongly in the UV, the number of scatterers contributing to the UV Raman signal may be very much smaller than that for the visible or near-IR signal. For example, with catalysts using TiO_2 as the support, the collected Raman scattered light under 244-nm excitation originates from a thin layer within 50 nm from the surface (37), whereas the visible Raman signal can be collected from a layer determined by the depth of field of the collection optics, typically 100 μm to a few hundred micrometers thick. In this case the number of scatterers contributing to the UV Raman signal, and hence the signal intensity, can be 10^{-4} to 10^{-3} smaller than with visible Raman measurements. Thus, signal intensities can be higher for visible Raman measurements when the catalyst support is strongly absorbing in the ultraviolet and visible wavelength excitation is preferred.

When compounds absorb UV photons, they may undergo laser-induced photochemistry. However, this effect can be minimized using the FB method for the measurement of Raman spectra. On the other hand, UV resonance Raman effect may occur under such conditions and this would improve detection sensitivity. UV resonance Raman spectroscopy may also be able to detect reaction intermediates at concentrations far below the detection limits of visible or near-IR Raman spectroscopy. Furthermore, in reactions with many different intermediates and products, one may identify certain functional groups or chromophores by selectively resonance enhancing these species using the appropriate UV excitation source. Because of the sensitivity and the ability of UV resonance Raman spectroscopy to identify specific functional groups, it is widely used in biology (38) where the molecule under study is often complex. This technique is not exploited at all in the field of heterogenous catalysis.

CONCLUSIONS

A novel fluidized bed technique for measuring UV Raman spectra of catalysts and adsorbates has been developed. Using this method, the adverse effects of UV radiation were minimized. This method should be applicable to a wide variety of catalytic systems and it can be adapted to perform *in situ* measurements under reaction conditions. It may also be used in other types of spectroscopies where sample damage due to the absorption of radiant energy is a major concern.

Although UV Raman spectroscopy is very useful in many instances, it will not replace visible Raman spectroscopy. These two techniques and near-IR Raman spectroscopy are complementary to one another. Depending on the experimental conditions and the desired results, one method may be preferred to the other two.

ACKNOWLEDGMENTS

We thank Amoco Oil Co. for providing the H-USY, H-ZSM-5, and naphthalene/H-USY samples. Financial support of this work was provided by the Department of Energy, Office of Basic Energy Sciences, Division of Chemical Sciences, under Contract DE-FG02-97ER14789.

REFERENCES

1. Dunn, J. P., Stenger, H. G., Jr., and Wachs, I. E., *J. Catal.* **181**, 233 (1999).
2. Scheithauer, M., Knözinger, H., and Vannice, M. A., *J. Catal.* **178**, 701 (1998).
3. Dutta, P. K., Mohana Rao, K., and Park, J. Y., *J. Phys. Chem.* **95**, 6654 (1991).
4. Brémard, C., and Bougeard, D., *Adv. Mater.* **7**, 10 (1995).
5. Dutta, P. K., *J. Incl. Phenom. Mol. Recogn. Chem.* **21**, 215 (1995).
6. Twu, J., Dutta, P. K., and Kresge, C. T., *Zeolites* **11**, 672 (1991).
7. Wechhuysen, B. M., Mestl, G., Rosynek, M. P., Krawietz, T. R., Haw, J. F., and Lunsford, J. H., *J. Phys. Chem. B* **102**, 3773 (1998).
8. Xie, S., Mestl, G., Rosynek, M. P., and Lunsford, J. H., *J. Am. Chem. Soc.* **119**, 10186 (1997).
9. Williams, C. T., Chen, E. K.-Y., Takoudis, C. G., and Weaver, M. J., *J. Phys. Chem. B* **102**, 4785 (1998).
10. Dutta, P. K., and Zaykoski, R. E., *Zeolites* **8**, 179 (1988).
11. Jeziorowski, H., and Knözinger, H., *Chem. Phys. Lett.* **51**, 519 (1977).
12. Hendra, P., Jones, C., and Warnes, G., "Fourier Transform Raman Spectroscopy: Instrumentation and Chemical Applications," p. 246. Ellis Horwood, New York, 1991.
13. Asher, S. A., and Johnson, C. R., *Science* **225**, 311 (1984).
14. Li, C., and Stair, P. C., *Catal. Lett.* **36**, 119 (1996).
15. Li, C., and Stair, P. C., *Catal. Today* **33**, 353 (1997).
16. Stair, P. C., and Li, C., *J. Vac. Sci. Technol. A* **15**, 1679 (1997).
17. Chan, S. S., and Bell, A. T., *J. Catal.* **89**, 433 (1984).
18. Wovchko, E. A., Yates J. T., Jr., Scheithauer, M., and Knözinger, H., *Langmuir* **14**, 552 (1998).
19. Lexel Laser, Inc., Fremont, CA.
20. Aero Research Associates, Inc., Port Washington, NY.
21. Newport, Corp., Irvine, CA.
22. OPCO Laboratory, Inc., Fitchburg, MA.
23. Cleveland Vibrator, Co., Cleveland, OH.
24. Mott, Corp., Farmington, CT.
25. Model 847, Eurotherm Controls, Inc., Reston, VA.
26. Knözinger, H., and Mestl, G., *Top. Catal.* **8**, 45 (1999), and references therein.
27. Stern, E. S., and Timmons, C. J., "Electronic Absorption Spectroscopy in Organic Chemistry," p. 115, 118, 145. St. Martin's Press, New York, 1971.

28. Dollish, F. R., Fateley, W. G., and Bentley, F. F., "Characteristic Raman Frequencies of Organic Compounds," p. 185, 162. Wiley, New York, 1974.
29. Kaye, W. I., *Appl. Spectrosc.* **15**, 130 (1961).
30. Blatter, F., Sun, H., and Frei, H., *Catal. Lett.* **35**, 1 (1995).
31. Yoshida, H., Tanaka, T., Yamamoto, M., Yoshida, T., Funabiki, T., and Yoshida, S., *J. Catal.* **171**, 351 (1997).
32. Tanaka, T., Matsuo, S., Maeda, T., Yoshida, H., Funabiki, T., and Yoshida, S., *Appl. Surf. Sci.* **121/122**, 296 (1997).
33. The size of the laser spot of $\sim$40 μm is determined by monitoring the intensity of the scattered photons while changing the entrance slitwidth of the Raman spectrometer. The laser spot size is found when the intensity is $(1 - 1/e^2)$ of the maximum. This occurs at a slitwidth of $\sim$1 mm. Knowing the magnification factors of our ellipsoidal mirror (9.8 to 24.6), we can then back-calculate to determine the laser spot size by dividing 1.0 mm by 24.6.
34. The depth of field of the ellipsoidal mirror at the sample position is determined by the change in Raman peak intensity of a sample by moving the latter from a position of maximum peak intensity to another position when the intensity has fallen to $(1 - 1/e^2)$ of the maximum. Twice of the distance between these two positions is the depth of field of the ellipsoidal collection mirror.
35. Ferraro, J. R., and Nakamoto, K., "Introductory Raman Spectroscopy," p. 183. Academic Press, San Diego, 1994.
36. Huang, Y., and Qiu, P., *Langmuir* **15**, 1591 (1999).
37. This value was estimated from optical skin depth, d($\sim$200 Å), of 250-nm photons in TiO_2. The value of the optical skin depth, d, is calculated from the equation $d = \lambda/2\pi k$, where λ is the wavelength of the excitation source, and k is the extinction coefficient obtained from the following references. (a) Joseph, J., and Gagnaire, A., *Thin Solid Films* **103**, 257 (1983). (b) Palik, E. D. (Ed.), "Handbook of Optical Constants of Solids," p. 795. Academic Press, New York, 1985.
38. Spiro, T. G. (Ed.), "Biological Applications of Raman Spectroscopy," Vol. 2. Wiley, New York, 1987.